*Quest Journals*
*Journal of Research in Environmental and Earth Science*
*Volume 3~ Issue 5 (2017) pp: 55-66*
*ISSN(Online) : 2348-2532*
www.questjournals.org

**Research Paper**

# Remote Sensing And Gis Application in Image Classification And Identification Analysis.

Gbola K. Adewuyi[1]*, Akeem A. Babatunde[2] and Stephen A. Aderinkomi[3]
*[1, 2, 3] Department of Surveying and Geoinformatics, Faculty of Environmental Studies,*
*The Polytechnic Ibadan, Oyo State, Nigeria.*
*Corresponding Author: Gbola K. Adewuyi[1]**

**R**eceived 14 October, 2017; **A**ccepted 28 October, 2017 © The author(s) 2017. **P**ublished with open access at **www.questjournals.org**

***ABSTRACT:*** *Remote sensing data play an important role in production of Land Use and Land Cover maps and this can therefore be managed through a process called image classification. Image classification is a way of allocating land cover classes into pixels while image identification/recognition is a way of detecting and identifying an object or a feature in a digital image. This paper examines image classification and identification using Remote Sensing and GIS. An unsupervised classification based method was used for this study which involved image interpretation using image processing software and separates a large number of unknown pixels based on their reflectance values into classes. The objective of image classification is to identify and portray, as a unique gray level (or color), the features occurring in an image in terms of the object or type of land cover these features actually represent on the ground. Three classes identify in this study are the Soil, Water and Vegetation. Landsat 8 ETM+ Satellite imagery with 512 x 512 dimension was used in classifying the image into class type. Further analysis on classification and identification was done using IDRISI 17.0 (selva edition) and ArcGIS 10.2 (Arcmap 10.2) software. Composite map that classify the pixel in the image and their corrected band, Graphical relationship between atmospheric effect and signal wavelengths of the bands for the extracted region selected and chart for the brightness value were produced. It was concluded that water has the highest percentage in volume than others.*

***Keywords:*** *Image Classification, image Recognition, land cover, Reflectance value, class type*

## I. INTRODUCTION

Image Classification is defined as the process of categorizing all pixels in an image or raw remotely sensed satellite data to obtain a given set of labels or land cover themes [1]. The purpose of the classification process is to group all pixels in a digital image into one of different land cover classes/themes. This grouped data can be used to produce thematic land cover maps present in an image. In a usual way, multi-spectral data are the best to use in carry out the classification. Indeed, the existing spectral pattern within the data for each pixel is used as the numerical basis for categorization [1]. The most important part of digital image analysis is image classification. A quality image shows a magnitude of colors illustrating various features of the underlying terrain. [2]. In image classification, supervised classification identifies the Information classes examples (i.e., land cover type) of interest in the image and these are known as training sites. A statistical characterization of reflectance for each information class will then be developed using image processing software and this stage is known as signature analysis stage and this involve the development of characterization as the rage of reflectance on each bands, or as complicated as comprehensive analyses of the mean, variances and covariance above all bands. Once a statistical characterization has been developed and achieved for each information class, then the image will be classified by examining the reflectance for each pixel and making a decision about which of the signatures it resembles most. [3]

Till this present time, regional land use land cover maps is required to produce for the variety of purposes of government, public, private, and national security applications besides to support regional landscape planning and resource management [4].However, there are two broad types of classification procedure and each finds application in the processing of remote sensing images: one is referred to as supervised classification and the other one is unsupervised classification. These can be used as alternative approaches, but are often combined into hybrid methodologies using more than one method [5].

[4] states that various classification approaches have been developed and widely used to produce land cover maps and are range in logic, from supervised to unsupervised; parametric to nonparametric to non-metric, or hard and soft (fuzzy) classification, or per-pixel, sub-pixel, and pre-field [6], [7].

Unsupervised image classification is a method in which the image interpreting software separates a large number of unknown pixels in an image based on their reflectance values into classes or clusters with no direction from the analyst [8].

Unsupervised classification is a method which examines a large number of unknown pixels and divides into a number of classes based on natural groupings present in the image values [9]. Besides, unsupervised classification is easy to apply, does not require analyst specified training data and is widely available in image processing and statistical software packages; moreover it automatically converts raw image data into useful information so long as there is higher classification accuracy [10], but one disadvantage of this classification is that the classification process has to be repeated if new data (samples) are added.

High results have been achieved using hybrid classification in a combination of unsupervised classifications (ISODATA) and Maximum likelihood as supervised to produce land cover maps by using multi-temporal Landsat images (TM) in Northeast Cairo, Egypt.[11]. Landsat 8 Operational Land Imager (OLI) and Thermal Infrared Sensor (TIRS) are instruments onboard the Landsat 8 satellite which was launched in February of 2013. The satellite gathered together images of the Earth with a 16-day repeat cycle, referenced to the Worldwide Reference System-2. The satellite's acquisitions are in an 8-day offset to Landsat 7 [12]. The approximate scene size is 170 km north-south by 183 km east-west (106 mi by 114 mi).

The spectral bands of the OLI sensor, while similar to Landsat 7's ETM+ sensor, provide enhancement from prior Landsat instruments, with the addition of two new spectral bands: a deep blue visible channel (band 1) specifically designed for water resources and coastal zone investigation, and a new infrared channel (band 9) for the detection of cirrus clouds. Two thermal bands (TIRS) capture data with a minimum of 100 meter resolution, but are registered to and delivered with the OLI data product. (See Landsat satellite band designations for more information.)

A multi-spectral sensor imageries example is Landsat 8 and it produces 11 images with the following bands:
Band 1: Coastal aerosol (0.43-0.45 um)
Band 2: Blue (0.45-0.51 um)
Band 3: Green (0.53-0.59 um)
Band 4: Red (0.64-0.67 um)
Band 5: Near infrared NIR (0.85-0.88 um)
Band 6: Short-wave Infrared SWIR 1 (1.57-1.65 um)
Band 7: Short-wave Infrared SWIR 2 (2.11-2.29 um)
Band 8: Panchromatic (0.50-0.68 um)
Band 9: Cirrus (1.36-1.38 um)
Band 10: Thermal Infrared TIRS 1 (10.60-11.19 um)
Band 11: Thermal Infrared TIRS 2 (11.50-12.51 um)
Each band has a spatial resolution of 30 meters with the exception of band 8, 10 and 11. Band 8 has a spatial resolution of 15 meters. Band 10 and 11 has spatial resolutions of 100 meters. Therefore, this study aimed at analyzing *number of unknown pixels based on their reflectance values into classes* using Remote Sensing And GIS Application.

## II. MATERIALS/METHODS

### 3.1 Materials

The material used for this study are both the hardware and software and they are;

#### *3.1.1 Hardware*

- *Laptop Computer*
- *32 gigabite hard drive*

#### *3.1.2 Software*

- Landsat Imagery
- Arc GIS 10.2 (ArcMAP)
- IDRISI 17.0
- Microsoft Word Office

### 3.2 Methods

The method adopted for this study was based on the use of LandSat 8 ETM+ imagery with the extraction of around 512 x 512 pixels containing Vegetation, Soil and Water were identified (fig. 10). Importation of the image to Idrisi 17.0 was done and selection of the GeoTIFF option, since the software version doesn't support Landsat-8 directly and the result of importation of image into IDRISI format for each Bands 2, 3, 4. Red, Green and Blue respectively were generated (fig. 1, 2, 3, 4, 5 ). Identification of each classes was done by carrying out the following;

- Training of signature class of extracted image.
- Making of signature file for each class trained.
- MAKESIG report for three feature classes trained. (fig. 8)
- Parallelepiped classification of extracted image with threshold values of Vegetation 30, Water 20 and Soil 25. (fig. 9)

Composite for bands 4,3,2 (true color) was done with a final dimension of 512 x 512 x 3. After performing parallelepiped classification based on the spectral signature reflectance, vegetation, water and soil classes were effectively identified (fig. 10). The classification showed that water had the highest percentage in volume.

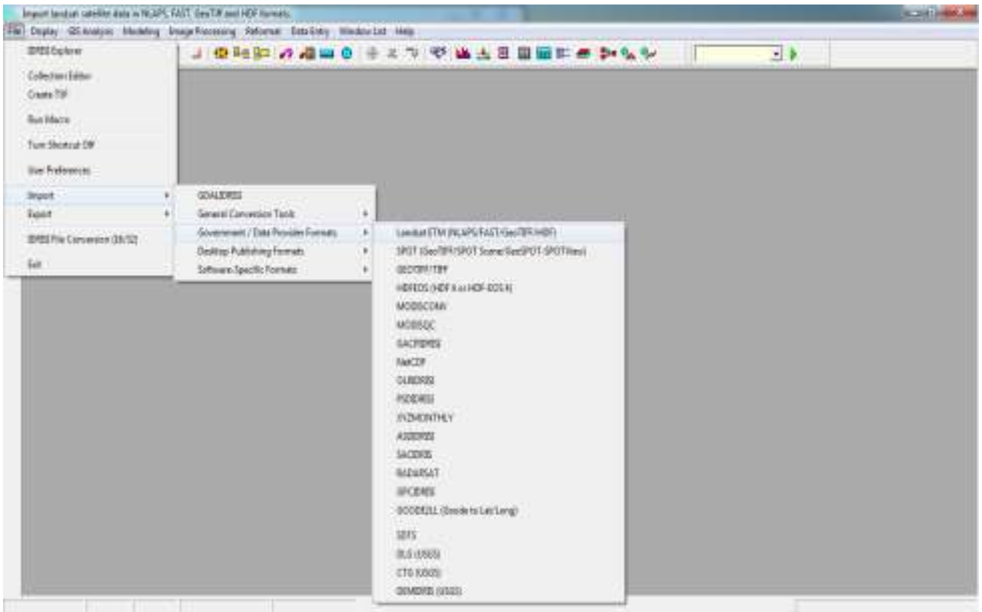

Figure 1: Importing of image into IDRISI software environment using the LANDSAT Government/Data Provider Formats.

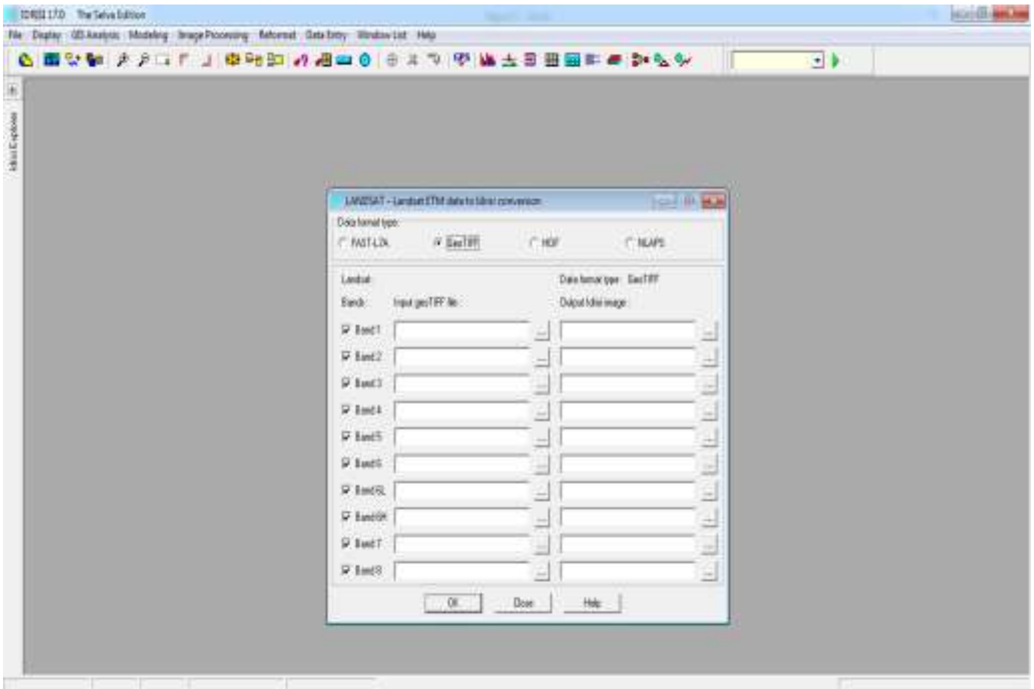

Figure 2: Selection of the GeoTIFF option, since the software version doesn't support Landsat-8 directly.

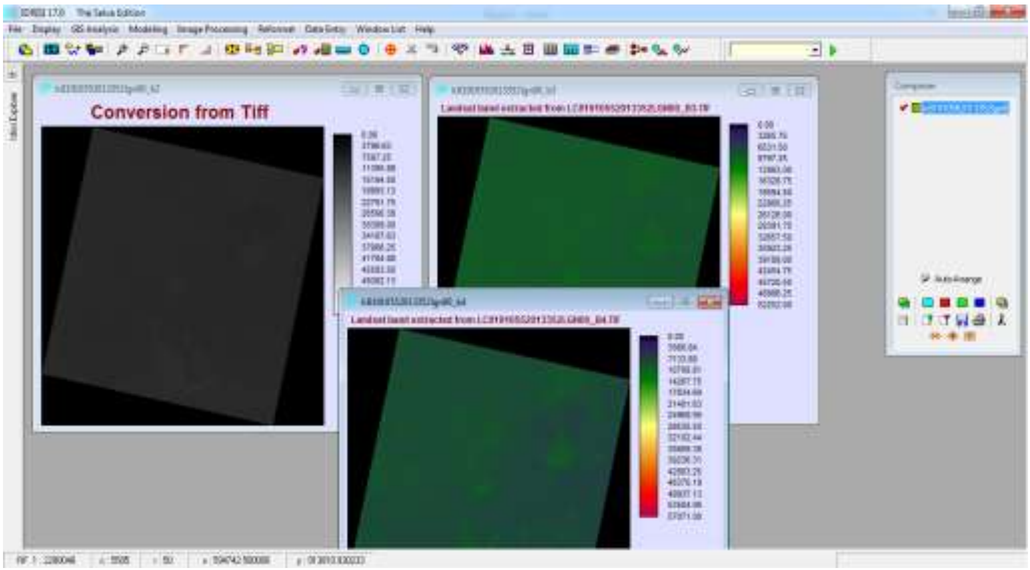

Figure 3: Result of importation of image into IDRISI format. Bands 2, 3, 4. Red, Green and Blue respectively.

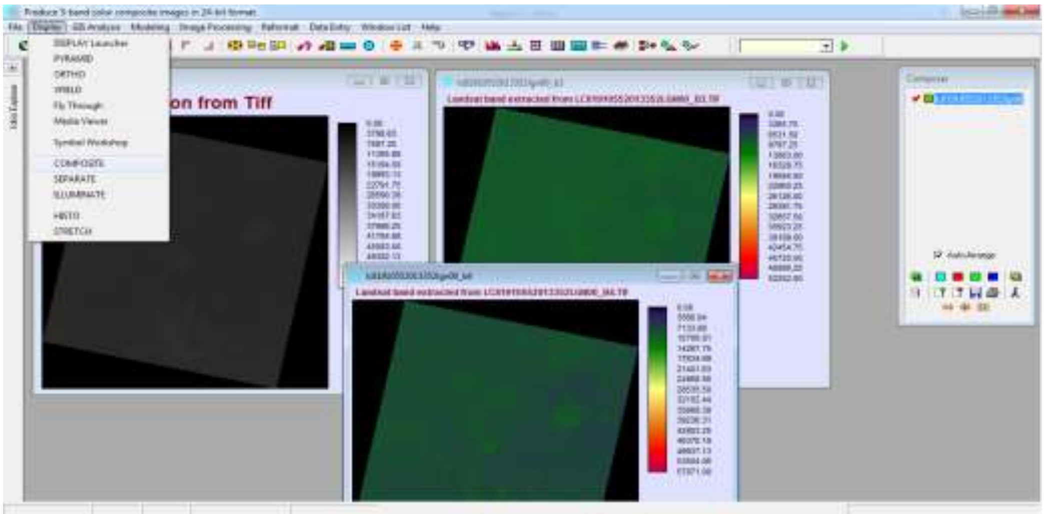
Figure 4: Composite of 4, 3, 2 in RGB channels, for true color combination.

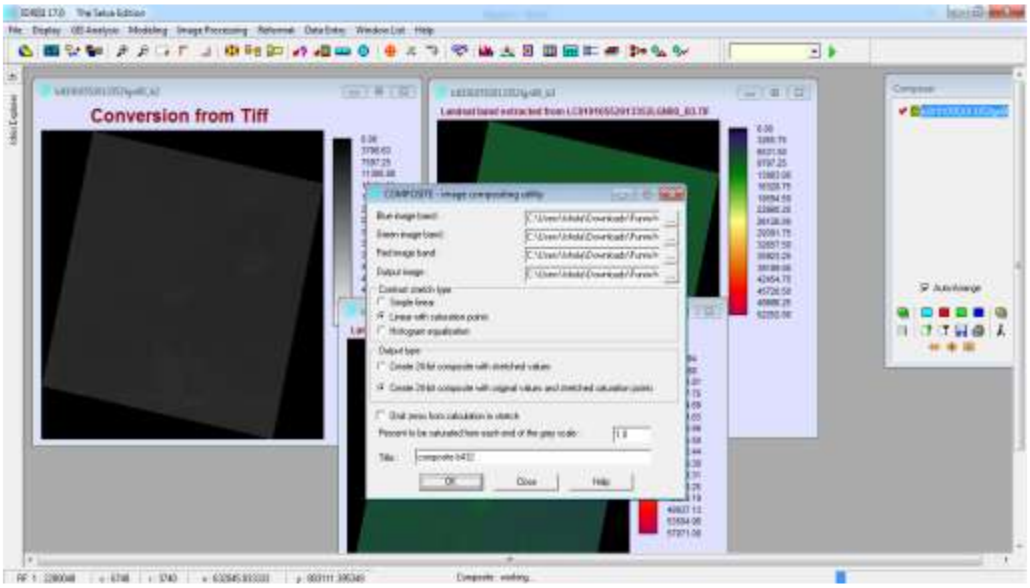

Figure 5: Composite generation.

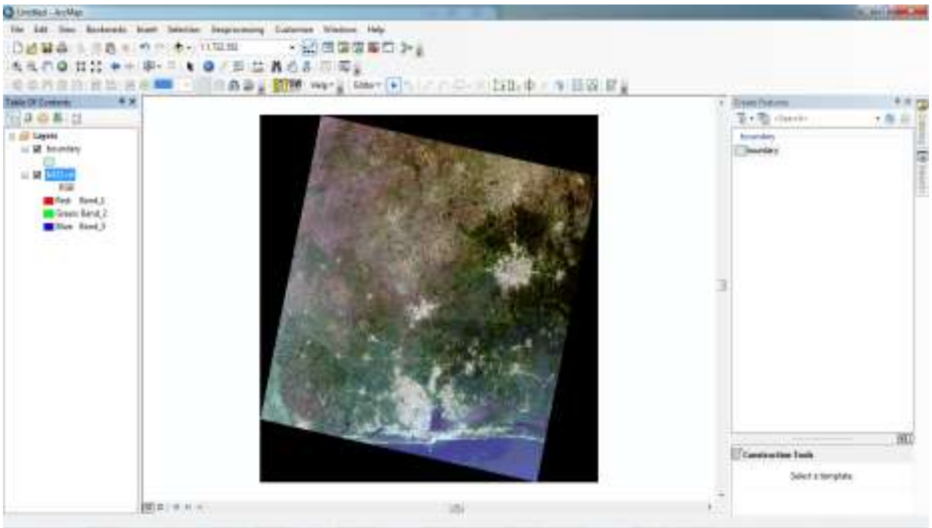

Figure 6: Composite image is loaded in the ArcGIS environment in order to clip out needed region.

Figure 7: Composite region clipped out.

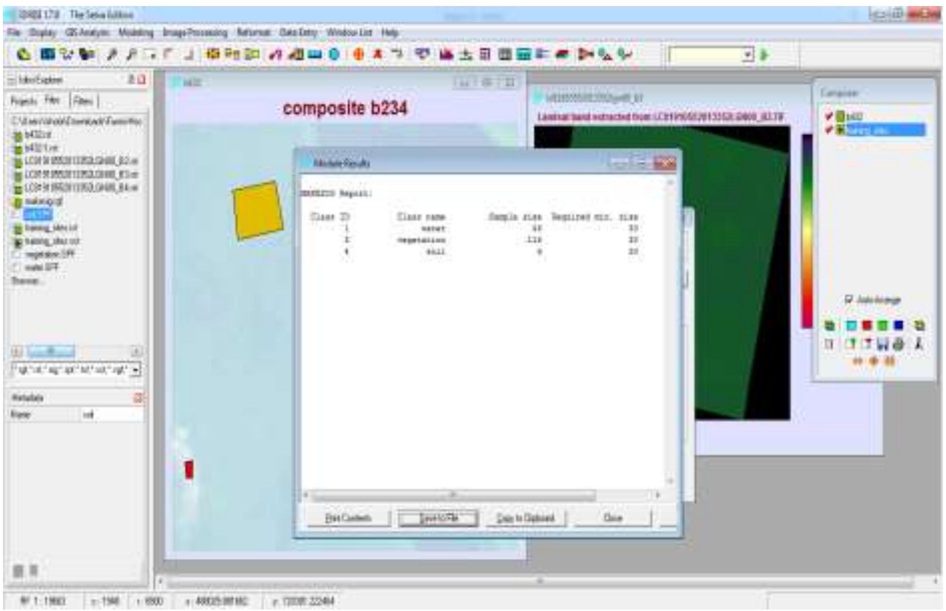


**Figure 8:** MAKESIG report for three feature classes trained.

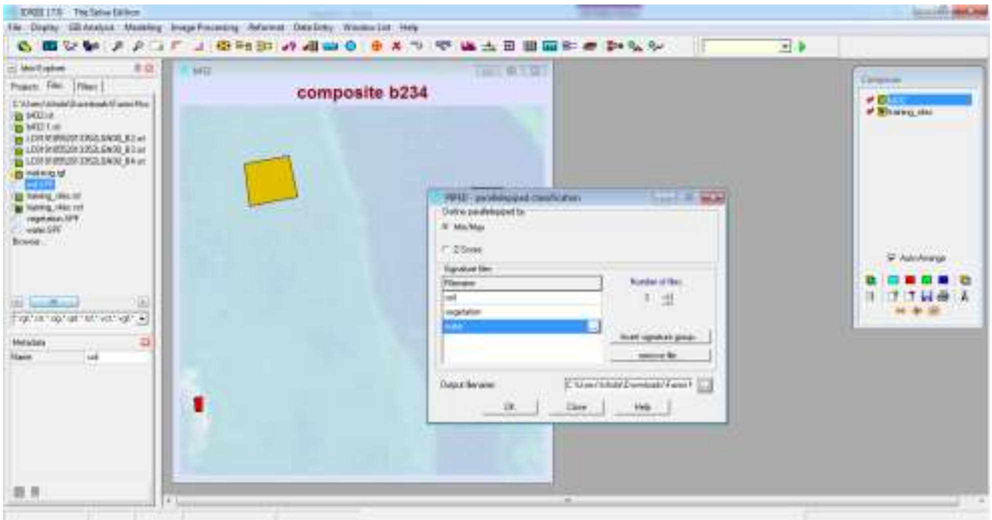


**Figure 9:** Parallelepiped classification with threshold values of Vegetation 30, Water 20 and Soil 25.

## III. RESULT AND ANALYSIS

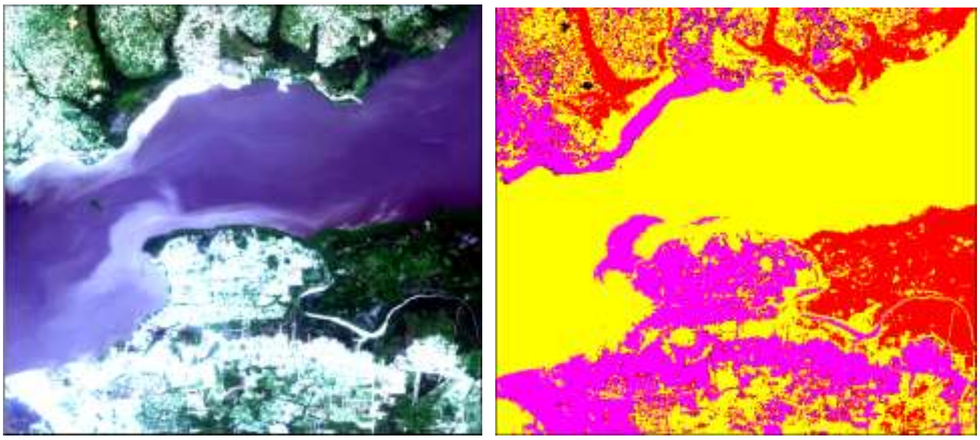

**Figure 10:** Side-by-side comparison/identification of spectral signature with Magenta as soil, Red as vegetation and Yellow as deep-shallow water.

Histogram of Number of pixels vs. Brightness value for each of the Blue, Green, Red and NIR bands extracted were drawn with class width of 20 ( fig. 11a-d). The graphic data type was generated and used to produce the histogram for each band.

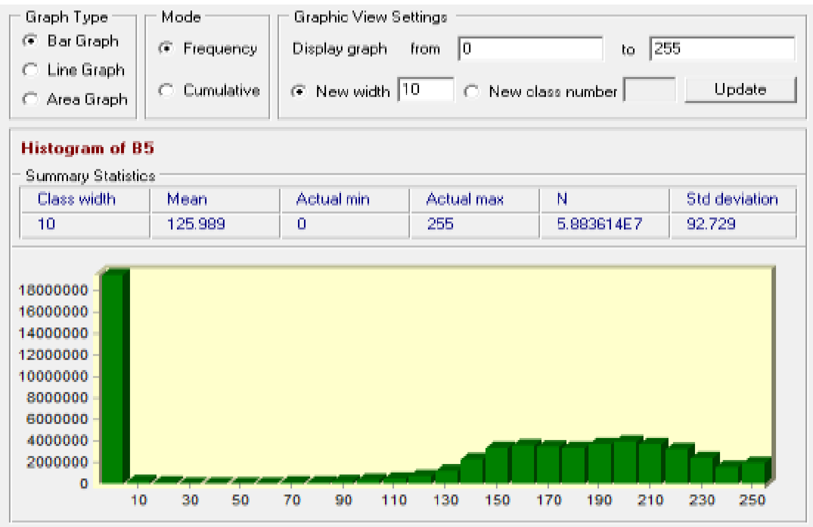


Figure 11a: Histogram for Band 5 at a Class width of 10.

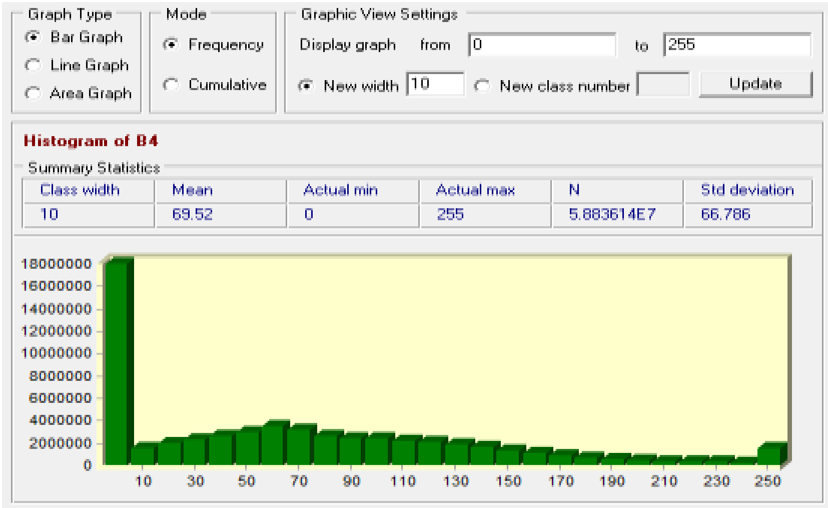


**Figure 11b:** Histogram for Band 4 at a Class width of 10.

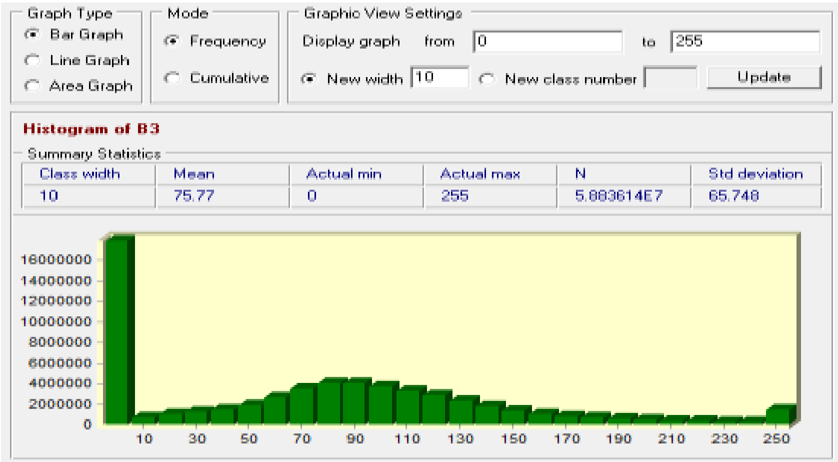


**Figure 11c:** Histogram for Band 3 at a Class width of 10

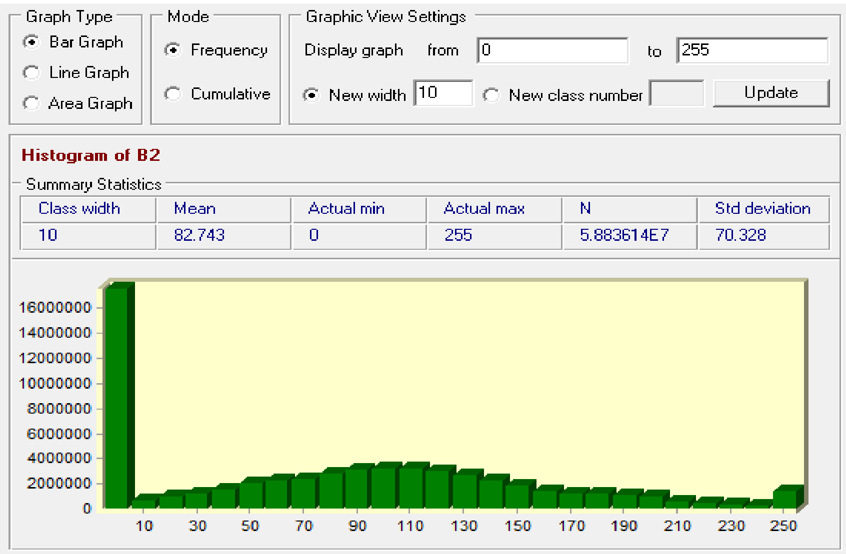


**Figure 11d:** Histogram for Band 2 at a Class width of 10.

The relationship between atmospheric effect and signal wavelength for an assumption of some pixels at or close to zero. And also determination of atmospheric effect corrections to each band and application of those corrections obtained were done.

Relationship between atmospheric effect and signal wavelength for the extracted bands was done. A spectral library was built for the bands of the extracted LandSat image and then with a wavelength unit in Nanometer. Below is a graphical representation that shows the relationship for the bands of their atmospheric effects and their signal wavelength in Nanometer. (Fig. 12)

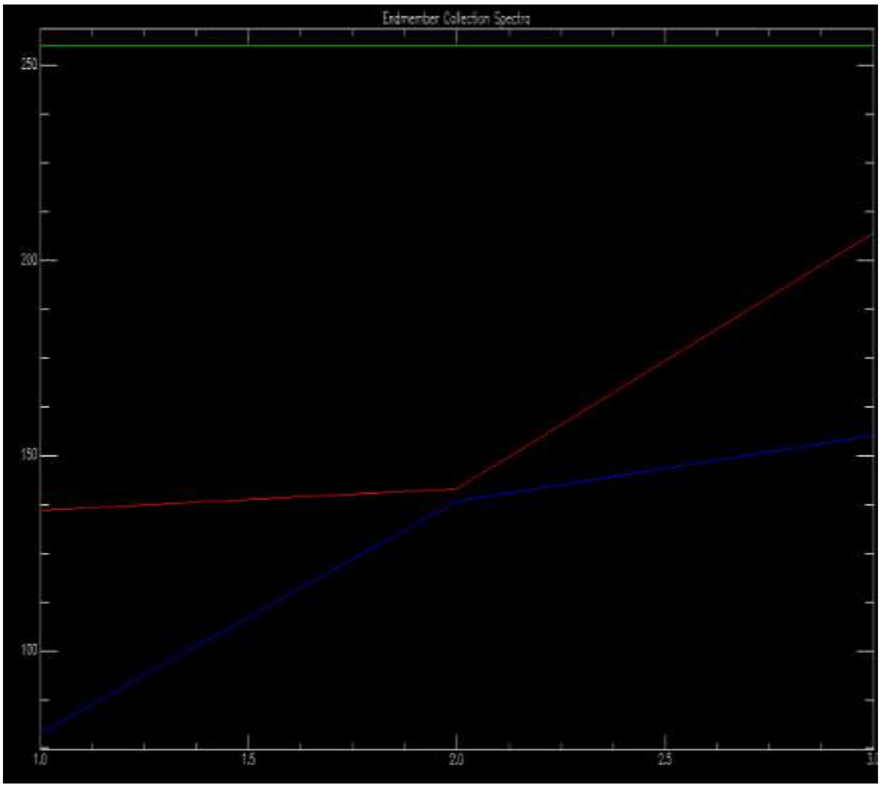


**Figure 12:** Graphical relationship between atmospheric effect and signal wavelengths of the bands for the extracted region selected.

Correction for atmospheric effect to be applied to each band and its application

The reflectance data ρ (λ)

$$\rho(\lambda_i) = \frac{\int \rho(\lambda)\, S_i(\lambda)\, d\lambda}{\int S_i(\lambda)\, d\lambda}$$

Radiance conversion of digital numbers can be achieved using sensor calibration coefficients. Digital number (DN) of satellite data was converted into spectral radiance (Li) using prelaunch calibration coefficients then the top of atmosphere (TOA) reflectance (ρ (λi)) for each spectral bands (figure 12a-d) were computed by converting spectral radiance to reflectance as,

$$\rho_{\lambda_i} = \frac{\pi L_i d^2}{E_o \, Cos\theta}$$

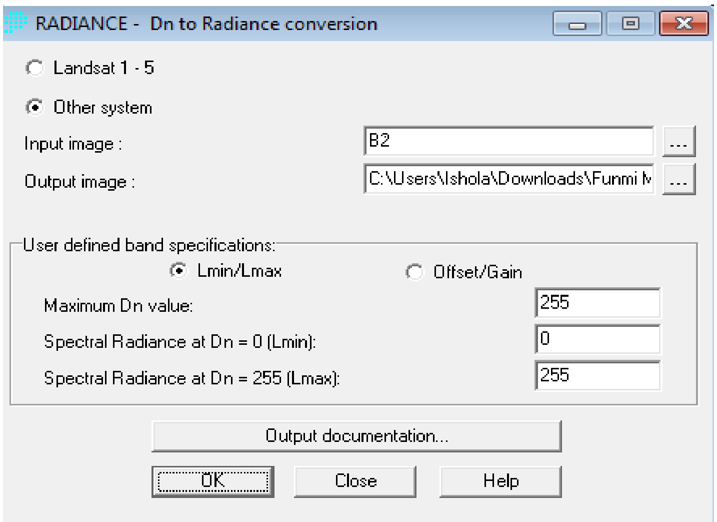

Figure 12a: Correction for band 2 (Blue) of extracted region using the Lmin/Lmax specifications.

Spectral radiance at DN = 0 (Lmin)
Spectral radiance at DN = 255 (Lmax)

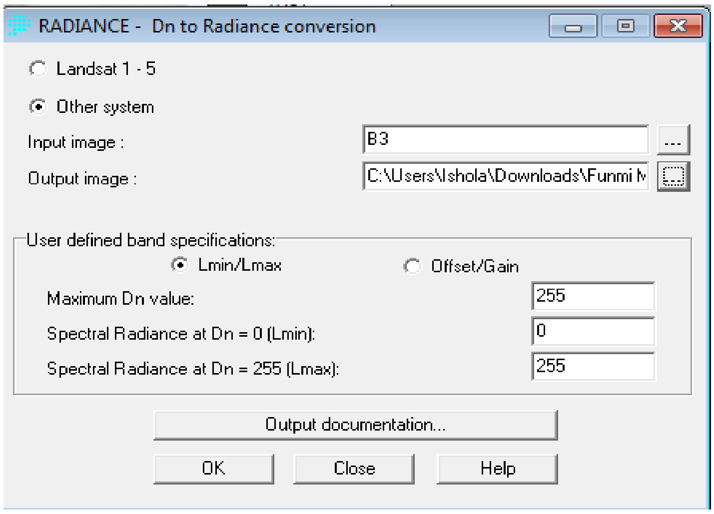

Figure 12b: Correction for band 3 (Green) of extracted region using the Lmin/Lmax specifications.

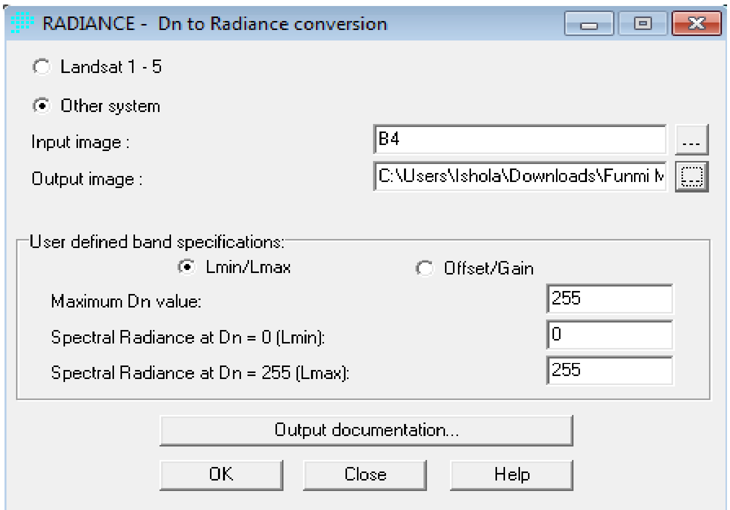

Figure 12c: Correction for band 4 (Red) of extracted region using the Lmin/Lmax specifications.

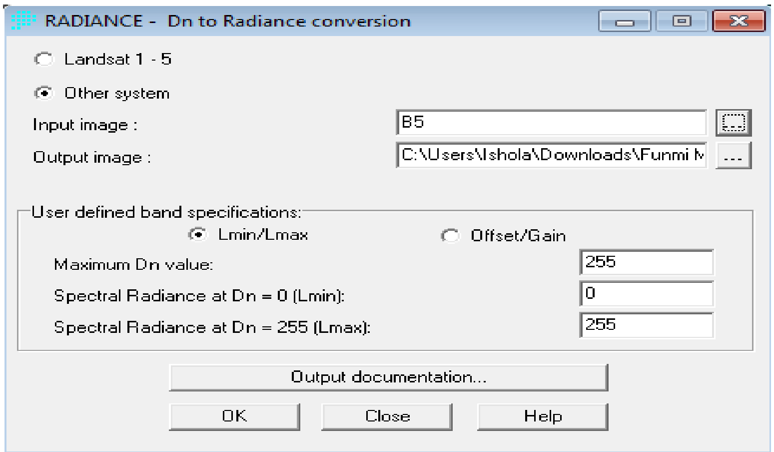


Figure 12d: Correction for band 5 (NIR) of extracted region using the Lmin/Lmax specifications.

Comments on visual identification on the classes

Figure 13: Corrected Original

From the (fig. 13) above for band 2 (Blue), it is observed that after the correction for atmospheric effects by conversion of the DN values to radiance, it is observed that the soil class is more enhanced being the brightest in visual appearance but the water feature is well distinguished.

**Figure 14:** Corrected Original

From the (fig 14) above for band 3 (Green), it is observed that after the correction for atmospheric effects by conversion of the DN values to radiance, it is observed the vegetation feature is well distinguished.

**Figure 15:** Corrected Original

From the (fig. 15) above for band 4 (Red), it is observed that after the correction for atmospheric effects by conversion of the DN values to radiance, it is observed the vegetation and soil feature is well distinguished.

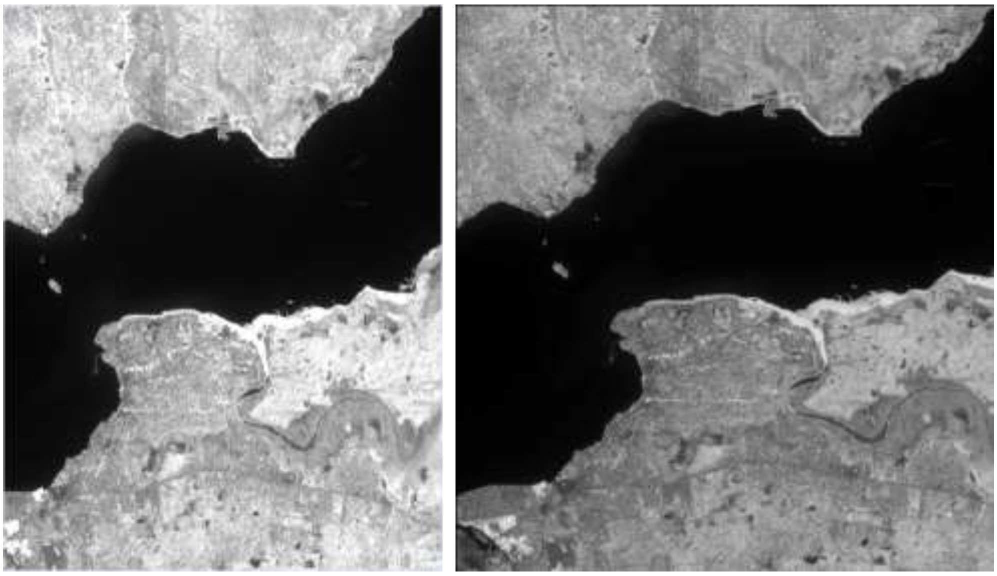

Figure 16: Corrected Original

From the (fig. 16) above for band 5 (NIR), it is observed that after the correction for atmospheric effects by conversion of the DN values to radiance, it is observed the vegetation feature is well distinguished as it has the best enhancement for visual interpretation.

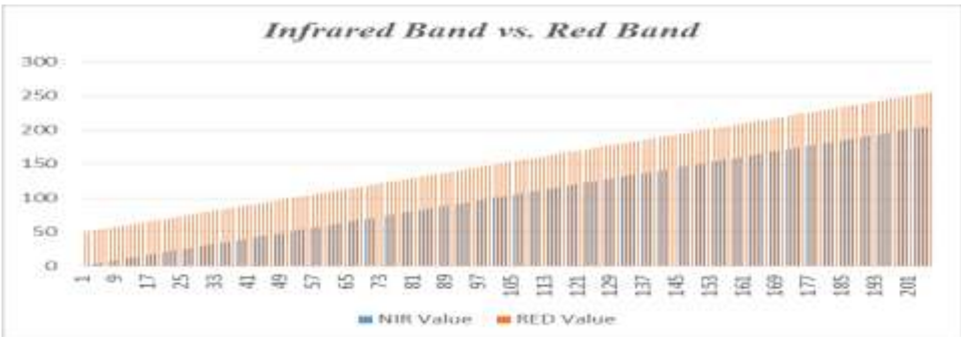


**Figure 17:** Brightness values of Infrared vs. Red Bands.

From (fig. 17) above, the pixel values of the infrared are higher. Also, compared to the grouping done in one, vegetation would be reflected more with the band 5 which is in the infrared region of the electromagnetic spectrum.

## IV. CONCLUSION

Remote sensing in production of Land Use / Land Cover maps is very important and this can be achieved through a process known as Image Classification. The use of Landsat imagery cannot be overemphasized in Image Classification and identification in the producing of surface land cover map at regional, national and international scale, multiple use of remote-sensing features information with spectral, spatial, multi-temporal, and Multi-sensor, building and use of an complex classification algorithms, such as pre-field, sub-pixel, and knowledge-based classification algorithms, and lastly embodied of ancillary data into classification processes, such as topography, soil, road, and census data. For this study, it can be concluded that Landsat image was use effectively to classify and identify each band and the correction made were used to distinguished one from the other for the selected classes (Soil, Water and Vegetation).

## V. RECOMMENDATIONS

The authors recommend the following;

- Landsat imagery should be employ in analysis of land use/land cover map
- The use of Geographical Information System and application software in production of new thematic map showing land cover/land use cover should be encouraged
- Applications of Land use cover should be encouraged by government, public, private, and national security to support regional landscape planning and resource management

## REFERENCES


[1]. Lillesand, T.M. & Keifer, R.W. Remote Sensing and Image Interpretation. 1994

[2]. PCI. Using PCI Software, PC1 Corp., Richmond Hill, Ontario, Canada, 551 p. 1997

[3]. Eastman J. R. Raster Procedures for Multi-Criteria/Multi-0biective Decisions PN ARTICTE Photogrammetric Engineering & Remote Sensing 61 (5), 1995, 539-547.

[4]. Aplin, P. & Atkinson, P.M. Predicting missing field boundaries to increase per-field classification accuracy, Photogrammetric Engineering and Remote Sensing, vol. 70, no. 1, 2004, pp. 141-149.

[5]. Richards, J.A. and Jia, X. Remote sensing digital image analysis: an introduction, Springer Verlag. 2006

[6]. Keuchel, J., Naumann, S., Heiler, M. and Siegmund, A. Automatic land cover analysis for Tenerife by supervised classification using remotely sensed data, Remote Sensing of Environment, vol. 86, no. 4, 2003a , pp. 530-541.

[7]. Jensen, J., "Introductory Digital Image Processing, 3rd", 2005.

[8]. Tou, J.T. and Gonzalez, R.C. Pattern recognition principles, Image Rochester NY, vol. 7. Vanderzee, D. & Ehrlich, D. 1995, "Sensitivity of ISODATA to changes in sampling procedures and processing parameters when applied to AVHRR time-series NDV1 data", Remote Sensing, vol. 16, no. 4, 1974, pp. 673-686.

[9]. Balasubramanian subbiah and seldevChristopher.c. Image classification through integrated K-means algorithm. IJCSI International Journal of Computer Science Issues, Vol. 9, Issue 2, No 2, 2012

[10]. Langley, S.K., Cheshire, H.M. & Humes, K.S., A comparison of single date and multitemporal satellite image classifications in a semi-arid grassland, Journal of Arid Environments, vol. 49, no. 2, 2001, pp. 401-411.

[11]. Zaki, R. & Abotalib Zaki, S.A., Land Use and Land Cover Changes in Arid Region: The Case New Urbanized Zone, Northeast Cairo, Egypt, Journal of Geographic Information System, vol. 3, no. 3, 2011, pp. 173-194.

[12]. http://landsat.usgs.gov/tools_acq.php. Introduction to Landsat 8


Gbola K. Adewuyi*. "Remote Sensing And Gis Application in Image Classification And Identification Analysis." Quest Journals Journal of Research in Environmental and Earth Science, vol. 03, no. 05, 2017, pp. 55–66.